

The Primordial Lithium Problem

BRIAN D. FIELDS

*Departments of Astronomy and of Physics, University of Illinois, Urbana IL
61801 USA*

Key Words big bang nucleosynthesis, early universe, dark matter, abundances of light elements, extensions of the Standard Model

Abstract Big-bang nucleosynthesis (BBN) theory, together with the precise WMAP cosmic baryon density, makes tight predictions for the abundances of the lightest elements. Deuterium and ^4He measurements agree well with expectations, but ^7Li observations lie a factor 3 – 4 below the BBN+WMAP prediction. This 4 – 5 σ mismatch constitutes the cosmic “lithium problem,” with disparate solutions possible. (1) Astrophysical systematics in the observations could exist but are increasingly constrained. (2) Nuclear physics experiments provide a wealth of well-measured cross-section data, but ^7Be destruction could be enhanced by unknown or poorly-measured resonances, such as $^7\text{Be} + ^3\text{He} \rightarrow ^{10}\text{C}^* \rightarrow p + ^9\text{B}$. (3) Physics beyond the Standard Model can alter the ^7Li abundance, though D and ^4He must remain unperturbed; we discuss such scenarios, highlighting decaying Supersymmetric particles and time-varying fundamental constants. Present and planned experiments could reveal which (if any) of these is the solution to the problem.

CONTENTS

Introduction	2
Standard BBN in Light of WMAP: the Lithium Problem Emerges	3
<i>Standard BBN Theory</i>	3
<i>Light Element Observations</i>	4
<i>Microwave Background Anisotropies as a Cosmic Baryometer</i>	6
<i>Assessing Standard BBN: the Lithium Problem(s) Revealed</i>	6
Solutions to the Lithium Problem(s)	7
<i>Astrophysical Solutions</i>	7
<i>Nuclear Physics Solutions</i>	9
<i>Solutions Beyond the Standard Model</i>	11
Discussion and Outlook	16
Disclosure Statement	16
Acknowledgments	17

arXiv:1203.3551v1 [astro-ph.CO] 15 Mar 2012

1 Introduction

Big bang nucleosynthesis (BBN) describes the production of the lightest nuclides—D, ^3He , ^4He , and ^7Li —at times ~ 1 sec to ~ 3 min after the big bang. Theoretical predictions of the light element abundances are well-understood and rest on the secure microphysics of nuclear cross sections and Standard Model weak and electromagnetic interactions (1,2). These predictions are in broad quantitative agreement with measured primordial light element abundances derived from observations in the local and high-redshift universe. This concordance represents a great success of the hot big bang cosmology, and makes BBN our earliest reliable probe of the universe.

BBN has dramatically changed over the past decade in response to the cosmological revolution sparked by the recent flood of new observations. Notably, WMAP measurements of the cosmic microwave background (CMB) radiation have precisely determined the cosmological baryon and total matter contents (3,4), while high-redshift supernova observations reveal that the universe recently entered a phase of accelerated expansion (5,6,7,8). These and other observations reveal the *existence* and tightly determine the *abundance* of both dark matter and dark energy on cosmic scales where they dominate the mass-energy budget of the universe today. Yet the nature of both dark matter and dark energy remains unknown. Thus 21st-century cosmology finds itself in a peculiar state of “precision ignorance;” this situation is particularly exciting for particle physics because both dark matter and dark energy demand physics beyond the Standard Model.

BBN has played a central role in the development of this new cosmology. CMB data now measure of the cosmic baryon density, independently of BBN, and with high precision. This casts BBN in a new light: a comparison of these two measures of cosmic baryons provides a strong new test of the basic hot big bang framework (9). Moreover, this test can now be performed in a new way, using the CMB baryon density as an *input* to the BBN calculation, which outputs predictions for each light element abundance; these can then each be directly compared to light element observations (10). The result is that deuterium shows spectacular agreement between BBN+CMB predictions and high-redshift observations, and ^4He shows good agreement. However, using the first-year WMAP data, ^7Li showed a discrepancy of a factor 2–3, representing a $2-3\sigma$ disagreement between observations and theory (11,12,13,14). This disagreement has worsened over time, now standing at a factor 3–4 in abundance or $4-5\sigma$: this is the “lithium problem.”

In this paper we present an overview of the lithium problem, accessible to nuclear and particle physicists and astrophysicists. Broader reviews of primordial nucleosynthesis and its relation to cosmology and particle physics are available (2,15,16,17).

In Section 2, we trace the origin of the lithium problem, with a focus on the physics of BBN ^7Li production, the nature and precision of light element abundance measurements, and the state of light element concordance in view of the CMB-measured cosmic baryon density. We review possible solutions to the lithium problem in Section 3: (i) astrophysical systematic uncertainties in lithium abundances and/or their interpretation; or (ii) new or revised nuclear physics inputs to the BBN calculation, in the form of increased mass-7 destruction via novel reaction pathways or by resonant enhancement of otherwise minor channels; or (iii) new physics – either particle processes beyond the Standard Model occur-

ring during or soon after BBN, or large changes to the cosmological framework used to interpret light element (and other) data. We close by summarizing the near-future outlook in Section 4.

2 Standard BBN in Light of WMAP: the Lithium Problem Emerges

2.1 Standard BBN Theory

The cosmic production of light nuclides is the result of weak and nuclear reactions in the context of an expanding, cooling universe. “Standard” BBN refers to the scenario for light element production which marries the Standard Model of particle physics with the “standard” (Λ CDM) cosmology, with:

1. gravity governed by General Relativity
2. a homogeneous and isotropic universe (cosmological principle)
3. the microphysics of the Standard Model of particle physics
4. the particle content of the Standard Model, supplemented by dark matter and dark energy

Under these assumptions, the expansion of the universe is governed by the Friedmann equation

$$\left(\frac{\dot{a}}{a}\right)^2 \equiv H^2 = \frac{8\pi}{3}G\rho \quad (1)$$

where $a(t)$ is the dimensionless cosmic scale factor (related to redshift z via $1+z = 1/a$), and $H = \dot{a}/a$ is the universal expansion rate. The total cosmic mass-energy density $\rho = \sum \rho_i$ sums contributions from all cosmic species i .

By far the largest contribution to the density comes from *radiation*: relativistic species for which $m \ll T$ (with T the temperature), namely blackbody photons and $N_\nu = 3$ species of neutrinos and antineutrinos, and e^\pm pairs at $T \gtrsim m_e$. Cosmic *matter* consists of nonrelativistic species with $m \gg T$: nucleons n and p , and e^- at $T \lesssim m_e$. Since $\rho_{\text{rad}} \gg \rho_{\text{matter}}$, eq. (1) shows that radiation dominates cosmic dynamics during BBN.

BBN occurs entirely in this radiation-dominated epoch, for which the energy density has $\rho \propto T^4$, where $T \propto 1/a$ (adiabatic cooling). This, together with eq. (1), gives $t \propto 1/T^2$, or

$$t \approx 1 \text{ sec} \left(\frac{1 \text{ MeV}}{T}\right)^2 \quad (2)$$

Light-element formation depends crucially on the relative amounts of baryons (nucleons) and radiation, parameterized by the baryon-to-photon ratio

$$\eta \equiv \frac{n_b}{n_\gamma} = 2.74 \times 10^{-8} \Omega_b h^2 \quad (3)$$

Here $\Omega_b = \rho_b/\rho_{\text{crit}}$ and $\rho_{\text{crit}} = 3H_0^2/8\pi G$, with H_0 the present expansion rate (Hubble parameter). In standard BBN, η is the *only* free parameter controlling primordial light element abundances.

Initially, cosmic baryons are in the form of free nucleons n and p . For $T \gtrsim 1$ MeV and thus $t \lesssim 1$ sec, weak interactions are rapid (rates per nucleon $\Gamma_{n \leftrightarrow p} \gg$

H) and thus

$$n\nu_e \leftrightarrow pe^- \quad (4)$$

$$p\bar{\nu}_e \leftrightarrow ne^+ \quad (5)$$

drive neutron and protons to an equilibrium ratio

$$\frac{n}{p} = e^{-(m_n - m_p)/T} \quad (6)$$

Thinking of the nucleon as a two-level system, this simply the Boltzmann ratio of the excited to ground state populations.

At $T = T_f \approx 1$ MeV, the $n - p$ interconversion (eq. 4) stop as the weak interaction “freezes out” ($\Gamma_{n \leftrightarrow p} \ll H$), fixing $n/p \approx e^{-(m_n - m_p)/T_f} \sim 1/6$. Deuterium production $p(n, \gamma)d$ occurs, but is stymied by the large number of photons per baryon $n_\gamma/n_b = 1/\eta \sim 10^9$, which leads to effective deuteron photodissociation by the $E_\gamma > B_d = 2.22$ MeV tail of the Planck distribution. During this time, free neutron decay reduces the neutron-to-proton ratio to $n/p \approx 1/7$.

At $T \approx 0.07$ MeV, blackbody photons become ineffective to photodissociate deuterium. The deuteron abundance rapidly rises, and from this all of the light elements are built via strong (i.e., nuclear) interactions. A simplified reaction network appears in Fig. 1, highlighting the reactions which dominate production of the light nuclides. In contrast to much of stellar nucleosynthesis, for BBN the number of key reactions is small and well-defined, and all of the important reactions have been measured in the laboratory at the relevant energies; no low-energy extrapolations are needed.

Figure 2 shows the standard BBN light-element abundances as a function of the single free parameter $\eta_{10} = 10^{10}\eta$ (eq. 3). The vertical yellow band is the WMAP η range (see §2.3). We see that the ${}^4\text{He}$ abundance is weakly sensitive to η (note that the zero is suppressed in the top-panel abscissa). In contrast, deuterium drops strongly with η and ${}^3\text{He}$ decreases substantially. The ${}^7\text{Li}$ abundance is plotted after ${}^7\text{Be}$ decay and thus sums both mass-7 species. ${}^7\text{Li}$ production dominates the mass-7 abundance in the low η regime of the plot, while ${}^7\text{Be}$ production dominates at the high- η regime, leading to the ‘dip’ behavior.

The envelopes around the curves in Fig. 2 correspond to the 1σ uncertainties in the abundance predictions. These uncertainties are propagated from the error budgets—statistical and systematic—of the twelve dominant reactions shown in Fig. 1 (18, 19, 20, 21, 22, 23, 24, 25, 26, 12). The uncertainties in ${}^4\text{He}$ are tiny ($< 1\%$), those in D and ${}^3\text{He}$ are small ($\sim 7\%$), while the ${}^7\text{Li}$ uncertainties are the largest ($\sim 12\%$ in the high- η regime of interest).

Several aspects of lithium production are noteworthy. Mass-7 is produced both as ${}^7\text{Li}$ and as ${}^7\text{Be}$; the ${}^7\text{Be} \xrightarrow{\text{EC}} {}^7\text{Li}$ electron capture occurs long after BBN ceases (27). The ${}^3\text{He}(\alpha, \gamma){}^7\text{Be}$ channel dominates ${}^7\text{Be}$ production. Destruction occurs via ${}^7\text{Be}(n, p){}^7\text{Li}$ followed by the rapid ${}^7\text{Li}(p, \alpha){}^4\text{He}$ reaction. Finally, ${}^6\text{Li}$ production in standard BBN is very small: ${}^6\text{Li}/\text{H} \simeq 10^{-14}$, or ${}^6\text{Li}/{}^7\text{Li} \lesssim 10^{-4}$ (28, 29).

2.2 Light Element Observations

Measuring the primordial abundance of any light element remains challenging. The BBN levels set at $z \sim 10^{10}$ are reliably accessible only in sites at $z \leq 3$ and

oftentimes $z \sim 0$. Other nucleosynthesis processes have intervened, as evidenced by the nonzero metallicity of all measured astrophysical systems. Thus one seeks to measure light elements in the most metal-poor systems, and then to obtain *primordial abundances* requires extrapolation to zero metallicity. Our discussion will follow closely recent treatments in refs. (30,31,32).

2.2.1 DEUTERIUM, HELIUM-3, HELIUM-4 Deuterium can be measured directly at high redshift. It is present in distant neutral hydrogen gas clouds which are seen in absorption along sightlines to distant quasars. At present there are seven systems with robust deuterium measurements (33,34,35,36,37,38). These lie around redshift $z \sim 3$ and have metallicity $\sim 10^{-2}$ of solar; thus deuterium should be primordial. For these systems,

$$\frac{\text{D}}{\text{H}} = (2.82 \pm 0.21) \times 10^{-5} \quad (7)$$

where the error has been inflated by a the reduced $\chi^2_\nu = 2.95$.

Helium-4 can be measured in emission from nearby metal-poor galaxies (extragalactic H II regions). The challenge is to reliably infer abundances at the needed $\lesssim 1\%$ level. Several recent analyses differ due to systematics in the extraction of abundances from nebular lines (39,40,41,42,43). The mass fraction of (40)

$$Y_p = 0.249 \pm 0.009 \quad (8)$$

has the largest and most conservative measure of the error budget; the allowed range overlaps with analyses of other groups.

Helium-3 is at present only accessible in our Galaxy’s interstellar medium (44). This unfortunately means it cannot be measured at low metallicity, and so its primordial abundance cannot be determined reliably (45); we will not use ^3He to constrain BBN.

2.2.2 LITHIUM-7 Lithium is measured in the atmospheres of metal-poor stars in the stellar halo (Population II) of our Galaxy. Due to convective motions, surface material in stars can be dragged to the hot interior where lithium is burned readily; this effect is seen in low lithium abundances in *cool* halo stars. Fortunately, the *hottest* (most massive) halo stars have thin convection zones, and show no correlation between lithium and temperature. We consider only lithium abundances in these stars.

Figure 3 shows lithium and iron abundances for a sample of halo stars (46). Li/H is nearly independent of Fe/H ; this flat trend is known as the “Spite plateau” in honor of its discoverers (47). But heavy elements such as iron (“metals”) *increase* with time as Galactic nucleosynthesis proceeds and matter cycles in and out of stars. Thus the Spite plateau indicates that most halo star lithium is uncorrelated with Galactic nucleosynthesis and hence, lithium is primordial.

Moreover, the Spite plateau *level* measures the primordial abundance. Thanks to a sustained effort of several groups (46,48,49,50,51,52,53,54,55,56), a large sample of halo stars have measured lithium abundances. The dominant error are systematic. A careful attempt to account for the full lithium error budget found (57)

$$\frac{\text{Li}}{\text{H}} = (1.23^{+0.68}_{-0.32}) \times 10^{-10} \quad (9)$$

with this 95%CL error budget dominated by systematics (see also §3.1).

Finally, it is encouraging to note that lithium has now been seen in stars in an accreted metal-poor dwarf galaxy. The Li/H abundances are consistent with Spite plateau, pointing to its universality (58).

2.2.3 LITHIUM-6 Due to the isotope shift in atomic lines, ${}^6\text{Li}$ and ${}^7\text{Li}$ are in principle distinguishable in spectra. In practice, the isotopic splitting is several times smaller than the thermal broadening of stellar lithium lines. Nevertheless, the isotopic abundance remains encoded in the detailed *shape* of the lithium absorption profile.

High-spectral-resolution lithium measurements in halo stars attain the precision needed to see isotope signatures. ${}^6\text{Li}$ detections have been claimed, in the range (46)

$$\frac{{}^6\text{Li}}{{}^7\text{Li}} \simeq 0.05 \quad (10)$$

Fig. 3 shows the inferred ${}^6\text{Li}/\text{H}$ abundance for some of these stars; its constancy with metallicity is strikingly reminiscent of the ordinary Spite plateau and similarly seems to suggest a primordial origin.

Lithium-6 observations remain controversial. It has been argued that stellar convective motions can alter the delicate lineshapes and mimic ${}^6\text{Li}$ (59). Thus there are only a few halo stars for which there is widespread agreement that ${}^6\text{Li}$ has even been detected. Thus, the conservative approach is to take the ${}^6\text{Li}$ observations as upper limits, though it is of interest to see what is required to explain the “ ${}^6\text{Li}$ plateau,” if it exists. Regardless, the isotopic searches confirm that most of primordial lithium is indeed ${}^7\text{Li}$.

2.3 Microwave Background Anisotropies as a Cosmic Baryometer

It is difficult to overstate the cosmological impact of the stunningly precise CMB measurements by WMAP and other experiments. The temperature and polarization anisotropies encode a wealth of cosmological information. Temperature fluctuations robustly record acoustic oscillations of the (re)combining baryon-photon plasma within dark matter potential; for a review, see (60). One of the most precise and robust results is the measurement of the cosmic baryon density and thus of η .

Figure 4 shows the sensitivity of the temperature anisotropy to the baryon density, as a function of angular scale (multipole) on the sky. Broadly speaking, increasing baryon density amplifies the odd peaks and depresses the even peaks. Accurate measurements of these peaks by WMAP and other experiments pins down the baryon density. The most recent 7-year WMAP data release gives

$$\eta = (6.19 \pm 0.15) \times 10^{-10} \quad (11)$$

a 2.4% measurement!

2.4 Assessing Standard BBN: the Lithium Problem(s) Revealed

Prior to WMAP, BBN was the premier means of determining the cosmic baryon density. Standard BBN has one free parameter, η , but three light elements have well-measured primordial abundances: D, ${}^4\text{He}$, and ${}^7\text{Li}$. Thus the problem is overdetermined: each element ideally selects a given value of η , but allowing for

uncertainties actually selects a range of η . If the different ranges are concordant, then BBN and cosmology are judged successful, and the cosmic baryon density is measured. This method typically specifies η to within about a factor ~ 2 (61,62).

The exquisite precision of the CMB-based cosmic baryon density suggests a new way of assessing BBN (9,10). We exploit the CMB precision by using η_{wmap} as an *input* to BBN. This removes the only free parameter in the standard theory. Propagating errors, we compute likelihoods for all of the light elements. Fig. 5 shows these likelihoods (30) based on WMAP data (63). Also shown are measured primordial abundances as discussed above.

Figure 5 shows that deuterium observations are in spectacular agreement with predictions—the likelihoods literally fall on top of each other. This concordance links $z \sim 3$ abundance measurement with $z \sim 10^{10}$ theory and $z \sim 1000$ CMB data, and represents a triumph of the hot big bang cosmology. We also see that ^4He predictions are in good agreement with observations. And, as noted in §2.2, no reliable primordial ^3He measurements exist.

Turning to ^7Li , the BBN+WMAP predictions and the measured primordial abundance completely disagree: the predictions are substantially *higher* than the observations. Depending on the treatment of systematic errors in the measured Li/H, the discrepancy is a factor $\text{Li}_{\text{bbn+wmap}}/\text{Li}_{\text{obs}} = 2.4 - 4.3$, representing a 4.2–5.3 σ discrepancy. This substantial mismatch constitutes the *lithium problem* (i.e., the ^7Li problem).

Finally, as noted in §2, standard BBN predicts an unobservable $^6\text{Li}/\text{H}$ abundance and $^6\text{Li}/^7\text{Li}$ ratio far below the putative ^6Li plateau. To the extent that the ^6Li plateau is real, this would constitute a second Li problem—the ^6Li problem.

Hereafter we will focus largely on the well-established ^7Li problem, but where appropriate we will mention the ^6Li problem.

3 Solutions to the Lithium Problem(s)

We have seen that the lithium problem was brought into sharp relief with the advent of the WMAP era, has become increasingly acute since. Possible solutions fall in three broad classes corresponding which part of the preceding analysis is called into question:

1. *Astrophysical* solutions revise the measured primordial lithium abundance.
2. *Nuclear Physics* solutions alter the reaction flow into and out of mass-7.
3. Solutions *beyond the Standard Model* invoke new particle physics or non-standard cosmological physics.

We consider each in turn.

3.1 Astrophysical Solutions

We first consider the possibility that BBN predictions are sound, i.e., standard cosmology and particle physics are correct, and the nuclear physics of mass-7 production is properly calculated. If so, then the measured value of the primordial lithium abundance must be in error. In particular, the true value must be higher by a factor 3–4.

As described in §2.2, lithium abundances are measured via absorption lines in the photospheres of primitive, low-metallicity stars. For each star, the lithium

line strength is used to infer the Li/H abundance. Lithium abundances are nearly insensitive to metallicity (Fig. 3)—this Spite plateau implies that lithium is independent of Galactic nucleosynthesis and is primordial, and the plateau level is taken as the primordial abundance. If missteps exist in this chain of reasoning, the lithium problem could potentially be alleviated.

For example, systematic errors could shift Li/H ratios in each star. We seek the *total* lithium content of the stellar photosphere, i.e., summed over all ionization states. However, the single (!) accessible 670.8 nm lithium line is sensitive only to neutral Li⁰. But in the stars of interest, lithium is mostly singly ionized. One must therefore introduce a large ionization correction Li⁺/Li⁰ that is exponentially sensitive to the stellar temperature. Thus, a systematic shift upward in the temperature scale for halo stars would increase all stellar Li abundances and raise the Spite plateau towards the BBN+WMAP prediction.

In practice, accurate determination of stellar temperatures remains non-trivial, because the emergent radiation is not a perfect Planck curve (else no lithium lines!), nor is local thermodynamic equilibrium completely attained in the stellar atmospheres. Quantitatively, the needed systematic shift in the temperature scale is about $\Delta T_{\text{eff}} \simeq 500 - 600$ K upward, a $\sim 10\%$ increase over fiducial values (outside of previous claimed errorbars) (64). A re-evaluation of one method to determine stellar temperatures indeed corrects the scale, typically by $\sim +200$ K (65). However, later detailed studies of the stellar temperature scale are in good agreement with the fiducial temperature scale, leaving the lithium problem unresolved (54, 66).

An entirely separate question remains as to whether a star's *present* lithium content reflects its *initial* abundance in the star. If the halo stars have destroyed some of their lithium, their present Li/H ratio sets a *lower limit* to the primordial lithium abundance. Indeed, given the low nuclear binding of ⁷Li, it need only be exposed to relatively low stellar temperatures ($T \gtrsim 2.5 \times 10^6$ K) to suffer substantial destruction over the many-Gyr lifespan of a halo star.

Lithium depletion is a major diagnostic of stellar structure and evolution (67, 68, 69, 70). For stars of *solar* composition, lithium destruction (71, 72) (72) has long been studied in stellar evolution models. The major effect is convection, which circulates photospheric material deep into the interior (though still far from the stellar core) where nuclear burning can occur. Models for the evolution of *low-metallicity* stars, appropriate for the Spite plateau, now include numerous mixing effects which can change the photospheric lithium: convective motions, turbulence, rotational circulation, diffusion and gravitational settling, and internal gravity waves (70, 73, 74, 75). These effects must occur at some level, and models have some success in fitting some observed trends in halo stars. There is general agreement that for stars with low metallicities, convective zones are substantially shallower than in solar-metallicity stars, and so depletion such be much smaller than the factor $\sim 10^2$ in the Sun (76). However, it remains difficult for models to quantitatively fit all of the data (49).

Thus *observational* efforts to find clues for lithium depletion in the Spite plateau stellar data themselves remain of utmost importance. One study found the Spite plateau in field halo stars to be very thin, with no detectable star-to-star variations around the Li-Fe trend, which showed a small positive slope in Li/H vs Fe/H (48). A small lithium increase with metallicity is *required* due to contamination from Galactic cosmic-ray production of ⁷Li and ⁶Li (57). An analysis of lithium and iron abundances in stars from the same globular cluster found trends con-

sistent with lithium depletion via diffusion and turbulent mixing; some models suggest these effects could remove the lithium problem entirely (50). However, systematic differences between globular cluster and field star lithium abundances raise concern about globular clusters at sites for constraining primordial lithium (56).

Recently, several groups have found that at *very* low metallicity, $[\text{Fe}/\text{H}] \lesssim -3$, lithium abundances on average fall *below* the Spite plateau (i.e., below the levels seen at metallicities $-3 \lesssim [\text{Fe}/\text{H}] \lesssim -1.5$) (52, 53, 51, 55). These groups also find that the star-to-star *scatter* in Li/H becomes significant below $[\text{Fe}/\text{H}] \lesssim -3$. This appears to confirm the presence of significant lithium depletion in at least some halo stars.

The recent evidence for lithium depletion at very low metallicities is a major development, yet its implications for primordial lithium remain unclear. No significant scatter is detected in plateau stars with $-3 \lesssim [\text{Fe}/\text{H}] \lesssim -1.5$. Also, in no stars is Li/H seen *above* the plateau, and in no metal-poor stars is Li/H near the WMAP+BBN value. Finally, while ${}^6\text{Li}$ measurements are difficult and controversial, there is general agreement that ${}^6\text{Li}$ is present in at least some plateau stars. This much more fragile isotope strongly constrains thermonuclear burning processes—if stellar material is exposed to temperatures hot enough to significantly reduce ${}^7\text{Li}$, ${}^6\text{Li}$ should be completely destroyed. (77).

To summarize, determination of the primordial lithium abundance continues to be the focus of rapid progress. At present, however, the observational status of primordial lithium remains unsettled. A purely astrophysical solution to the lithium problem remains possible. On the other hand, the observed lithium trends—particularly the small lithium scatter in temperature and metallicity, and the presence of ${}^6\text{Li}$ —strongly constrain (but do not rule out) solutions of this kind. Consequently, it is entirely possible that the lithium problem *cannot* be resolved astrophysically, and thus we are driven to seek other explanations of the discrepancy; we now turn to these.

3.2 Nuclear Physics Solutions

We now consider the possibility that the measured primordial lithium abundance is correct, and the Standard Model of particle physics and the standard cosmology are also sound. In this case, the lithium problem must point to errors in the BBN light element predictions, in the form of incorrect implementation of standard cosmological and/or Standard Model physics.

However, the standard BBN calculation is very robust and thus difficult to perturb. As summarized in §2, standard BBN rests on very well-determined physics applied in a very simple system. The cosmological framework of BBN is that of a very homogeneous universe (guaranteed by the smallness of the observed CMB temperature fluctuations (3)), with a cosmic expansion governed by exact expressions in General Relativity. The microphysics is that of the Standard Model, also very well-determined. The relativistic species, which comprise cosmic radiation that dominates the energy density, are very well thermalized and thus their properties are that of Bose-Einstein and Fermi-Dirac gasses, for which exact expressions are also available.

The weak and strong (i.e., nuclear) interactions are also well-grounded in theory and calibrated empirically, but for BBN the needed physics is complicated (nuclear networks are large) and lies the farthest from first principles. Thus,

these are the only possible “weak links” in the standard BBN calculation, and it is here that solutions to the lithium problem have been sought.

3.2.1 NEW AND REVISED REACTIONS One possibility is that weak and nuclear reactions in the BBN calculations are miscalculated due to reactions that are entirely missing, or that are included but whose rates are incorrect. But as described in §2 and seen in Fig. 1, only a relatively small number of reactions have been found to be important for producing the light elements, and all of these have been measured in the laboratory at the relevant energies. Their uncertainties have also been calculated and propagated through the BBN code, and are folded into the likelihoods appearing in Fig. 5. Moreover, BBN calculations use a much more extended reaction network than the simplified view of Fig. 1, with all initial state pairings of $A \leq 7$ species present but most practice unimportant (78, 79, 23, 80, 81, 82, 83). Thus, to change the primordial lithium predictions requires surprises of some kind—either (i) the cross sections the known important reactions have uncertainties far beyond the quoted errors, or (ii) the cross sections for normally unimportant reactions have been vastly underestimated.

For the important reactions seen in Fig. 1, mass-7 production is dominated by the single reaction ${}^3\text{He}(\alpha, \gamma){}^7\text{Be}$. While the quoted error budget in the measured cross section is small, $\sim 7\%$ (84), absolute cross sections are difficult to measure. However, this reaction is also crucial in the production of solar neutrinos. To fix the cosmic lithium problem, the ${}^3\text{He}(\alpha, \gamma){}^7\text{Be}$ normalization would need to be low by a factor 3–4; if this were the case, the ${}^7\text{Be}$ and ${}^8\text{B}$ solar neutrino fluxes would be lower by a similar factor. Thus we can view the sun as a reactor which probes the ${}^3\text{He}(\alpha, \gamma){}^7\text{Be}$ rate, and the spectacular and precise agreement between solar neutrino predictions and observations becomes a measurement of the rate normalization which confirms the experimental results and removes this as a solution to the lithium problem (85).

Weak rates in BBN have received a great deal of attention over the years (86, 87, 88, 89, 90, 91, 92, 93, 94). The basic $n \leftrightarrow p$ interchange rates (eq. 4) are most accurately normalized to the neutron lifetime. Corrections to the tree-level rates have $\lesssim 1\%$ effects on abundances, and thus are far too small to impact the lithium problem (94).

Corrections to the standard thermonuclear rates have been considered as well. The effects of nonthermal daughter particles has been studied and found to be negligible (95, 82). Plasma effects, and electron Coulomb screening are also unimportant (96).

Turning then to (normally) subdominant reactions, Angulo et al. (97) noted that the (nonresonant) cross section for ${}^7\text{Be}(d, \alpha)\alpha p$ was poorly determined and could solve the lithium problem if it were a factor ~ 100 larger. They measured the cross section at BBN energies, but found values a factor ~ 10 *smaller* than had been used.

Finally, the possibility of entirely new reactions has been recently studied by Boyd et al. (82). These authors systematically considered a large set of reactions, some of which have been neglected in prior calculations. The focus of this study is almost exclusively on nonresonant reactions, with the result that even when allowing for extremely large systematic uncertainties in known cross sections, most new channels remain unimportant. The loophole to this analysis is the presence of new or poorly measured resonances.

3.2.2 RESONANCES Both standard and nonstandard reaction pathways to primordial mass-7 are firmly anchored to experimental data. The only remaining new nuclear physics can only intervene via resonances which have evaded experimental detection or whose effects have been underestimated. Cyburt and Pospelov (98) point out that the production of the known resonance ${}^7\text{Be} + d \rightarrow {}^9\text{B}^*(16.71 \text{ MeV})$ is poorly constrained experimentally; this reaction appears in Fig. 1. Within current uncertainties, this resonance could promote the ${}^7\text{Be} + d$ channel to become the dominant ${}^7\text{Be}$ destruction mode, and solving the lithium problem in an elegant manner.

Generalizing the Cyburt and Pospelov (98) suggestion, ref. (99) searched the entire resonance solution space for BBN. These authors systematically considered all compound states created in mass-7 destruction, via all possible 2-body reactions of the form $(n, p, d, t, {}^3\text{He}, {}^4\text{He}) + ({}^7\text{Li}, {}^7\text{Be})$. Most possibilities were found to be unimportant. However, in addition to the ${}^7\text{Be} + d \rightarrow {}^9\text{B}^*(16.71 \text{ MeV})$ resonance, two other potentially important states were identified. The ${}^7\text{Be} + t \rightarrow {}^{10}\text{B}^*(18.80 \text{ MeV})$ resonance is known and within present uncertainties could be significant. On the other hand, there is little data on high-lying states of ${}^{10}\text{C}$, but if a ${}^{10}\text{C}^*(15.0 \text{ MeV})$ exists and has $J^\pi = 1^-$ or 2^- , this also could bring cosmic lithium into concordance if the reaction widths are large enough. This last possibility would be a homage to Fred Hoyle’s celebrated prediction of the ${}^{12}\text{C}^*(7.65)$ state which solved the “carbon problem” of stellar nucleosynthesis (100).

Fortunately all of these states are experimentally accessible. To identify or exclude them marks the endgame for a nuclear solution to the lithium problem.

3.3 Solutions Beyond the Standard Model

Finally, we turn to the most radical class of solutions the lithium problem. Namely, we assume that primordial lithium has been correctly measured, and that the nuclear physics of BBN has been calculated correctly and holds no surprises. In this case, we are forced to question the assumptions underlying the standard BBN calculation, i.e., we must go beyond the Standard Model of particle physics and/or the standard cosmology. For details beyond the overview below, see refs. (16, 15).

3.3.1 DARK MATTER DECAY AND SUPERSYMMETRY The existence of dark matter is now well-established, and its cosmic abundance has been inferred precisely; for recent reviews, see refs. (101, 102, 103). If dark matter takes the form of a relic particle created in the very early universe, it must be nonbaryonic. No Standard Model particles have the right properties, and thus dark matter *demands* physics beyond the Standard Model. Dark matter must of course be present during BBN, but ordinarily is assumed to be both nonrelativistic and weakly interacting, hence unimportant to cosmic dynamics and microphysical interactions. Similarly, dark energy is assumed to be negligible.

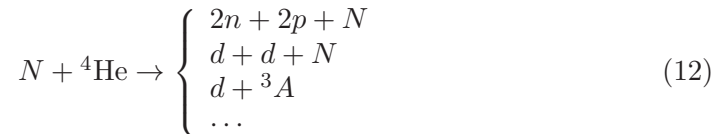
While the identity of the dark matter is unknown, a simple, popular, and physically well-motivated possibility is that dark matter today consists of relic weakly interacting massive particles (WIMPs). In particular, if the universe begins with equal abundances of WIMPs and anti-WIMPs (if the two are distinct), then their abundance today is determined by the freezeout of their annihilations. Famously, to reproduce $\Omega_m \simeq 0.3$ today, the annihilations must occur at $\sim \text{TeV}$ scales (well before BBN). By happy coincidence, this is also the scale of the weak interaction, and of current accelerator experiments—this is the “WIMP miracle”

(101, 102, 103).

Moreover, it is likely that WIMPs today are the stable endpoints of a decay cascade. If so, then the WIMPs are the daughters born in the decays of the next-lightest particles in the cascade. The nature of these decays is model-dependent, but in general produce Standard Model particles which interact with the background plasma. If the decays occur during or after BBN, the interactions can change light element abundances (104, 105, 106, 107, 108, 109, 110, 111, 112, 113, 114, 115, 116, 117), and thus potentially could solve the lithium problem(s) (118, 119, 120, 121, 122, 123, 124, 32).

We thus consider the effects of decaying massive particles during or after BBN. To get a feel for the basic physics, consider a particle X (and \bar{X} if they are distinct) with mass $m_X \gg m_p$, which decays with lifetime τ_X . The decays can have electromagnetic and/or hadronic channels, and given the massive nature of X , these decay products will be very relativistic and thus nonthermal.

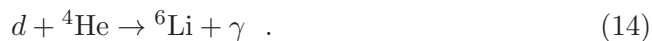
As these electromagnetic and/or hadronic cascades thermalize in the cosmic environment, they interact with the light elements, largely via fragmentation (photodissociation or spallation). For example, high energy nucleons N fragment ${}^4\text{He}$:



This reduces the ${}^4\text{He}$ abundance, but more importantly creates new deuterium and ${}^3\text{He}$. Furthermore, the secondary particles in eq. (12) are themselves nonthermal, and can initiate further interactions with the background thermal light nuclides. Of particular importance is the conversion of ${}^7\text{Be}$ into ${}^7\text{Li}$ with secondary neutrons



which substantially enhances mass-7 destruction because of the lower Coulomb barrier for ${}^7\text{Li}$. Also of interest is the nonthermal production of ${}^6\text{Li}$ via secondary nonthermal deuterons



Clearly, both of these processes are of great interest for both lithium problems.

Figure 6 shows light-element abundances in the presence of a hadronically decaying particle X . Abundance contours are plotted as a function of decay lifetime τ_X , and the pre-decay X abundance

$$\zeta_X \equiv \frac{m_X n_X}{n_\gamma} = m_X \frac{n_X}{n_b} \eta \quad (15)$$

In the absence of X decays, cosmic expansion dilutes baryons and X particles in the same way, and thus ζ_X remains constant. Figure 6 is for a hadronic branching fraction $B_h = 1$, i.e., all decays produce hadrons.

In each panel of Fig. 6, the colored areas indicate parameter regions where the predicted light element abundances disagree with observations, while the remaining white regions are allowed. At fixed τ_X , the light element perturbation is proportional to the X abundance. The limit $\zeta_X \rightarrow 0$ lies at the bottom of the plot, and corresponds to the unperturbed (standard BBN) case. At fixed abundance ζ_X , the light element effects strongly depend on particle lifetime, which determines when the light elements are perturbed. For example, at $\tau_X \lesssim 10$

sec, decays occur before the light elements are formed, and so the light elements are unaffected. Hadronic decays dominate the perturbations in the $\tau_X \lesssim 10^6$ sec of most interest here; electromagnetic decays dominate at longer times.

In the ${}^7\text{Li}/\text{H}$ panel, the colored regions include the unperturbed low- ζ_X regime, reflecting the lithium problem for standard BBN. However, for a relatively narrow region with lifetimes $\tau_X \sim 10^2 - 10^3$ sec, that the ${}^7\text{Li}$ abundance is reduced and brought into accord with observation. This arises due to the production of secondary neutrons (eq. 12), which facilitate mass-7 destruction via ${}^7\text{Be}$ -to- ${}^7\text{Li}$ conversion (eq. 13); at longer lifetimes the secondary neutrons decay. For $10^2 - 10^3$ sec lifetimes to be viable, however, the other light elements must remain in concordance. As seen in the final, summary panel, in the regime in which ${}^7\text{Li}$ is reduced, all other constraints are satisfied *except* D/H , which is unacceptably high due to secondary deuteron production. This tension between deuterium and ${}^7\text{Li}$ is a fundamental feature of decay scenarios, and as we see may allow for solutions but requires fine tuning.

Supersymmetry provides well-motivated candidates for decaying dark matter (125, 126, 127). Supersymmetry doubles the particle content of nature by requiring opposite-statistics (fermion \leftrightarrow boson) partners for every known particle. These partners are produced copiously in the very early universe. The lightest supersymmetric partner (LSP) is the stable end product of the decays of higher-mass supersymmetric particles, and naturally becomes a dark matter candidate (128, 129). These decays are a fundamental aspect of supersymmetric dark matter, and thus supersymmetric scenarios *demand* that particle decays occur. Moreover, even in the simplest scenarios—i.e., the constrained minimal supersymmetric Standard Model—the lifetime of the next-to-lightest supersymmetric partner can be long: $\gtrsim 100$ sec. Thus, minimal supersymmetry holds the tantalizing possibility of solving the lithium problem.

Figure 7 illustrates the interplay between supersymmetry and the lithium problem (32). The context is minimal supersymmetry in which the spin-3/2 gravitino is the next-to-lightest partner, which decays into the LSP neutralino that comprises the dark matter today. For a benchmark scenario in this model, the superpartner mass spectrum, lifetimes, and decay products are calculated. These are used to compute light element abundances, with nuclear uncertainties propagated; the results are compared to observations. The resulting χ^2 is plotted as a function of gravitino mass $m_{3/2}$ and pre-decay abundance $\zeta_{3/2}$. At low $\zeta_{3/2}$, we recover the unperturbed, standard case, where $\chi^2 \approx 32$ for one effective degree of freedom (3 light elements $-$ 2 parameters), a poor fit. At high $\zeta_{3/2}$, the light element perturbations are *worsened* over the standard case, and these supersymmetric parameters are excluded by BBN. Most interestingly, along the diagonal loop, the fit improves, and in the interior “islands,” χ^2 drops below 6, corresponding to $\sim 2.4\sigma$. This region shows substantial improvement over standard BBN, and physically arises as the regime of optimal tradeoff between ${}^7\text{Li}$ destruction and deuterium production. This region thus tantalizingly stands as a possible supersymmetric solution to the lithium problem, albeit statistically marginal and fine-tuned.

Finally, in very recent years an entirely new aspect of decaying dark matter alteration of BBN has emerged. If the decaying particles are electrically charged, then the negatively charged dark matter can form bound states with charged nuclei, such as (pX^-) , $({}^4\text{He}X^-)$, and $({}^7\text{Be}X^-)$. As pointed out by Pospelov

(117), these bound states unleash a rich array of new effects, in addition to the perturbations accompanying X^- decays. For the heavy X^- of interest, the binding energy of $(A^Z X^-)$ is $B = Z^2 A \alpha^2 m_p / 2 \approx 30 Z^2 A \text{ keV}$, comparable to nuclear binding. The Bohr radius is $a = (2\alpha Z A m_p)^{-1} \approx 1 A^{-1} Z^{-1} \text{ fm}$, comparable to nuclear sizes. Bound-state Coulomb barriers are thus reduced and $({}^7\text{Be}X^-)$ becomes easier to destroy.

Beyond these basic effects, a new “bound state chemistry” can occur, whose nature is still under active study. One important effect (117) is catalysis, particularly $d + ({}^4\text{He}X) \rightarrow {}^6\text{Li} + X$ which enhances ${}^6\text{Li}$ production far above the ordinarily small radiative capture $d(\alpha, \gamma){}^6\text{Li}$. This can enhance ${}^6\text{Li}$ production by orders of magnitude, possibly addressing the ${}^6\text{Li}$ problem if real, but oftentimes overproducing ${}^6\text{Li}$. Rates for catalyzed reactions have recently been calculated to high precision (130). Intriguingly, $({}^8\text{Be}X^-)$ states have a binding energy very close to the energy for ${}^8\text{Be} \rightarrow \alpha\alpha$ breakup; if the binding energy is larger, then $({}^8\text{Be}X^-)$ is stable and can allow for cosmological production of ${}^9\text{Be}$ (122, 131).

The general properties of X^- recombination and bound states, and their impact on BBN, have been studied in refs. (117, 132, 123, 133, 122, 15). Looking at bound state effect only (i.e., ignoring decay effects), catalyzed ${}^7\text{Be}$ destruction is effective and catalyzed ${}^6\text{Li}$ is not *over*produced, for sufficiently large X^- abundance in the regime $\tau_X \sim 2000 \text{ sec}$ (132). Indeed, there exist regions of parameter space wherein *both* the ${}^7\text{Li}$ and ${}^6\text{Li}$ problems are solved. Full calculation of bound state and decay effects together is required to verify if solutions remain in specific detailed models; early calculations confirm solution space exists around $\tau_X \sim 10^3$ (134, 123).

Catalyzed production of ${}^9\text{Be}$ also occurs and is constrained by the non-observation of a beryllium “Spite plateau;” the resulting limits on τ_X are comparable to those imposed by limits on primordial ${}^6\text{Li}$ (122). ${}^9\text{Be}$ constraints have the added advantage that they rely on elemental abundances which are much simpler to obtain reliably than isotopic abundances. However, very recently ${}^9\text{Be}$ was investigated using updated catalysis rates from ref. (130), which greatly reduce the ${}^9\text{Be}$ production rate. The resulting ${}^9\text{Be}$ abundance then is quite small, below observable levels (131).

Bound-state effects are important in the context of minimal supersymmetry. Substantial parameter space exists in which the gravitino is the LSP and thus the dark matter, while the next-to-lightest partner is the charged stau $\tilde{\tau}^\pm$, the scalar partner to the tau lepton. These models are probed by bound-state BBN, which imposes constraints that are complementary to accelerator limits (121, 132, 135, 133, 134, 122, 124, 136). Indeed, the solutions to the ${}^7\text{Li}$ and possibly also the ${}^6\text{Li}$ problem which exist at $\tau_X \sim 1000 \text{ sec}$ could be interpreted as support for these models.

To summarize, decaying dark matter scenarios introduce a rich array of novel processes that can alter light elements during and after BBN. Moreover, such scenarios find well-motivated origin in supersymmetric cosmologies. Indeed, decaying-particle BBN offers important constraints on supersymmetry. Furthermore, the ${}^7\text{Li}$ and possibly also ${}^6\text{Li}$ problems can be solved in decaying particle scenarios which are realized in plausible minimal supersymmetric scenarios. This area is ripe for further theoretical, observational, and experimental development.

3.3.2 CHANGING FUNDAMENTAL CONSTANTS Observations of multiple atomic transitions in metals residing in high-redshift quasar absorption systems test fun-

damental physics in environments at great spacetime separations from our own; for a review see ref. (137). Surprisingly, some data hint at variations in the fine-structure constant at $z \sim 3$, showing $\delta\alpha_{\text{EM}}/\alpha_{\text{EM}} \simeq -0.5 \times 10^{-5}$ at the $\sim 5\sigma$ level, while others find results consistent with no variation. Thus the observational situation is unsettled, but intriguing.

Time variations in low-energy physics can be accommodated and are even expected in the context of some unified theories which in general predict stronger variations at earlier times. Moreover, an underlying unified theory implies that all Standard Model couplings and particle masses should vary, with definite but model-dependent interrelationships.

There is thus theoretical impetus, and some observational motivation, to contemplate changes in fundamental constants during BBN. The change in light elements depends on which parameters (couplings, masses) change, and on the size of the perturbations (138,139,140,141,142). In general, there is large model-dependence in quantifying these variations, the links among them, and their manifestation in nuclear properties (masses, binding energies, cross sections).

An alternative approach is to turn the problem around and to consider the BBN implications of variation in nuclear physics parameters (143,144). Coc et al. (140) systematically study the light-element response to variations in α_{EM} , the electron mass m_e , the neutron lifetime τ_n , the neutron-proton mass difference $m_n - m_p$, and the deuteron binding energy B_D . Of these, the most sensitive parameter is the deuteron binding energy. A change of $-0.075 \lesssim \delta B_D/B_D \lesssim -0.04$ lowers the ${}^7\text{Li}$ abundance into concordance, without perturbing ${}^4\text{He}$ or D/H beyond their observed error range. Thus, unified models which predict changes of this order can solve the lithium problem.

3.3.3 NONSTANDARD COSMOLOGIES The lithium problem could indicate nonstandard cosmology rather than particle physics. One recent such proposal is that cosmic acceleration could result from large-scale inhomogeneities in the cosmic density. Isotropy constraints can be satisfied if we occupy a privileged view from nearly the center of a spherically symmetric cosmic underdensity, which only returns to the cosmic mean at horizon-scale distances (145). Such a scenario explains cosmic acceleration within General Relativity, and without invoking dark energy, but must abandon the cosmological principle, instead requiring that ours is a privileged view of the universe.

Esthetics aside, observations probe such an inhomogeneous cosmos. BBN occurs differently in such a universe, if the baryon-to-photon ratio varies along the inhomogeneity. In particular, ref. (146) emphasizes that the observations of ${}^7\text{Li}$ are made *locally*, at low z , while D/H and the CMB are both measured in the distant universe at high z . If the local baryon-to-photon ratio η_0 is low by a factor ~ 2 , then indeed one would expect local ${}^7\text{Li}$ to fall below the WMAP prediction, while D/H would agree.

This clever scenario however must face an array of observational tests. Relaxed galaxy clusters probe the cosmic baryon-to-matter fraction, and show variations $\lesssim 8\%$ out to $z \sim 1$, far less than the $\sim 50\%$ variation needed for lithium abundances (147). Moreover, local measurements of D/H even more directly constrain the local η measurement. Because some stellar destruction may well have occurred, the local D/H sets a lower limit to the primordial abundance. In the lower halo of our own Galaxy, $\text{D/H} = (2.31 \pm 0.24) \times 10^{-5}$. This value is in good agreement with the high- z D/H measurements and the WMAP+BBN

predictions; it is therefore inconsistent with the low η needed for a low local ${}^7\text{Li}/\text{H}$.

Other nonstandard cosmology scenarios have been proposed to solve the lithium problem. One suggests that a large fraction ($\sim 1/3 - 1/2$) of baryons were processed through the first generation of stars (Population III) which ejected lithium-free matter (148). Such models face great difficulties due to the substantial D/H depletion and ${}^3\text{He}$ production which must also occur (149, 150).

4 Discussion and Outlook

BBN has entered the age of precision cosmology. This transition has brought triumph in the spectacular agreement between high-redshift deuterium and the BBN+WMAP prediction, and in the WMAP confirmation of the longstanding BBN prediction of nonbaryonic dark matter. But new precision has raised new questions: the measured primordial ${}^7\text{Li}$ abundance falls persistently and significantly below BBN+WMAP predictions. Moreover, there are controversial hints of a primordial ${}^6\text{Li}$ abundance orders of magnitude above the standard prediction.

As we have seen, disparate explanations for the lithium problem(s) remain viable. Fortunately, most alternatives are testable in the near future.

1. *Astronomical observations.* Recent indications of lithium depletion in extremely metal-poor halo stars are tantalizing. In the coming Great Survey era, we may expect many more such stars to be identified, and the lithium trends explored in large statistical samples. These will require careful comparison with theory. Observations of ${}^6\text{Li}$ remain challenging, and as yet it remains unclear what trends exist with metallicity.

Great insight would result from alternative measures of primordial lithium, e.g., in the interstellar medium of metal-poor galaxies nearby or at high redshift.

2. *Nuclear experiments.* The enormous effort of the nuclear community has empirically pinned down nearly all nuclear inputs to BBN. Remaining are a few known or proposed resonances which would amplify ${}^7\text{Be}$ destruction. These are within reach of present facilities, so that the nuclear physics of standard BBN can and will be fully tested.
3. *Collider and dark matter experiments.* The LHC is operational and much of minimal supersymmetry lies within its reach. The discovery of supersymmetry would revolutionize particle physics and cosmology, and would transform decaying particle BBN scenarios into canonical early universe cosmology. Alternatively, if the LHC fails to find supersymmetry and/or finds surprises of some other kind, this will represent a paradigm shift for all of particle physics and particle cosmology, and BBN will lie at the heart of this transformation.

5 Disclosure Statement

The author is unaware of any affiliations, memberships, funding, or financial holdings that might be perceived as affecting the objectivity of this review.

6 Acknowledgments

It is a pleasure to thank my collaborators in primordial nucleosynthesis and closely related areas: Nachiketa Chakraborty, Richard Cyburt, John Ellis, Feng Luo, Keith Olive, Tijana Prodanović, Evan Skillman, Vassilis Spanos, and Gary Steigman. I am particularly grateful to Keith Olive for comments on an earlier version of this paper.

LITERATURE CITED

1. Wagoner RV, Fowler WA, Hoyle F, *Ap. J.* 148:3 (1967).
2. Steigman G, *Annu. Rev. Nucl. Part. Sci.* 57:463 (2007), 0712.1100.
3. Spergel DN, Verde L, Peiris HV, Komatsu E, Nolte MR, et al., *Ap. J. Supp.* 148:175 (2003), arXiv:astro-ph/0302209.
4. Larson D, Dunkley J, Hinshaw G, Komatsu E, Nolte MR, et al., *ArXiv e-prints* (2010), 1001.4635.
5. Riess AG, Filippenko AV, Challis P, Clocchiatti A, Diercks A, et al., *Astron. J.* 116:1009 (1998), arXiv:astro-ph/9805201.
6. Perlmutter S, Aldering G, Goldhaber G, Knop RA, Nugent P, et al., *Ap. J.* 517:565 (1999), arXiv:astro-ph/9812133.
7. Tonry JL, Schmidt BP, Barris B, Candia P, Challis P, et al., *Ap. J.* 594:1 (2003), arXiv:astro-ph/0305008.
8. Wood-Vasey WM, Miknaitis G, Stubbs CW, Jha S, Riess AG, et al., *Ap. J.* 666:694 (2007), arXiv:astro-ph/0701041.
9. Schramm DN, Turner MS, *Rev. Mod. Phys.* 70:303 (1998), arXiv:astro-ph/9706069.
10. Cyburt RH, Fields BD, Olive KA, *Astropart. Phys.* 17:87 (2002), arXiv:astro-ph/0105397.
11. Cyburt RH, Fields BD, Olive KA, *Phys. Lett. B* 567:227 (2003), astro-ph/0302431.
12. Cyburt RH, *Phys. Rev. D* 70:023505 (2004), astro-ph/0401091.
13. Coc A, Vangioni-Flam E, Descouvemont P, Adahchour A, Angulo C, *Ap. J.* 600:544 (2004), arXiv:astro-ph/0309480.
14. Cuoco A, Iocco F, Mangano G, Miele G, Pisanti O, Serpico PD, *International Journal of Modern Physics A* 19:4431 (2004), arXiv:astro-ph/0307213.
15. Pospelov M, Pradler J, *Annu. Rev. Nucl. Part. Sci.* 60:539 (2010), 1011.1054.
16. Jedamzik K, Pospelov M, *New J.Phys.* 11:105028 (2009), 0906.2087.
17. Iocco F, Mangano G, Miele G, Pisanti O, Serpico PD, *Phys. Rep.* 472:1 (2009), 0809.0631.
18. Krauss LM, Romanelli P, *Ap. J.* 358:47 (1990).
19. Smith MS, Kawano LH, Malaney RA, *Ap. J. Supp.* 85:219 (1993).
20. Fiorentini G, Lisi E, Sarkar S, Villante FL, *Phys. Rev. D* 58:063506 (1998), arXiv:astro-ph/9803177.
21. Hata N, Scherrer R, Steigman G, Thomas D, Walker T, et al., *Phys. Rev. Lett.* 75:3977 (1995), hep-ph/9505319.
22. Nollett KM, Burles S, *Phys. Rev. D* 61:123505 (2000), arXiv:astro-ph/0001440.
23. Cyburt RH, Fields BD, Olive KA, *New Astron.* 6:215 (2001), astro-ph/0102179.

24. Coc A, Vangioni-Flam E, Descouvemont P, Adahchour A, Angulo C, *Ap. J.* 600:544 (2004), astro-ph/0309480.
25. Descouvemont P, Adahchour A, Angulo C, Coc A, Vangioni-Flam E, *Atomic Data and Nuclear Data Tables* 88:203 (2004), arXiv:astro-ph/0407101.
26. Serpico PD, Esposito S, Iocco F, Mangano G, Miele G, Pisanti O, *J. Cosmol. Astropart. Phys.* 12:10 (2004), arXiv:astro-ph/0408076.
27. Khatri R, Sunyaev RA, ArXiv e-prints (2010), 1009.3932.
28. Thomas D, Schramm DN, Olive KA, Fields BD, *Ap. J.* 406:569 (1993), arXiv:astro-ph/9206002.
29. Vangioni-Flam E, Casse M, Cayrel R, Audouze J, Spite M, Spite F, *New Astron.* 4:245 (1999), arXiv:astro-ph/9811327.
30. Cyburt RH, Fields BD, Olive KA, *J. Cosmol. Astropart. Phys.* 11:12 (2008), 0808.2818.
31. Cyburt RH, Ellis J, Fields BD, Luo F, Olive KA, Spanos VC, *J. Cosmol. Astropart. Phys.* 10:21 (2009), 0907.5003.
32. Cyburt RH, Ellis J, Fields BD, Luo F, Olive KA, Spanos VC, *J. Cosmol. Astropart. Phys.* 10:32 (2010), 1007.4173.
33. Burles S, Tytler D, *Ap. J.* 507:732 (1998), arXiv:astro-ph/9712109.
34. Burles S, Tytler D, *Ap. J.* 499:699 (1998), arXiv:astro-ph/9712108.
35. O'Meara JM, Tytler D, Kirkman D, Suzuki N, Prochaska JX, et al., *Ap. J.* 552:718 (2001), arXiv:astro-ph/0011179.
36. Kirkman D, Tytler D, Suzuki N, O'Meara JM, Lubin D, *Ap. J. Supp.* 149:1 (2003), arXiv:astro-ph/0302006.
37. O'Meara JM, Burles S, Prochaska JX, Prochter GE, Bernstein RA, Burgess KM, *Ap. J. Lett.* 649:L61 (2006), arXiv:astro-ph/0608302.
38. Pettini M, Zych BJ, Murphy MT, Lewis A, Steidel CC, *Mon. Not. Roy. Astr. Soc.* 391:1499 (2008), 0805.0594.
39. Olive KA, Skillman ED, *New Astron.* 6:119 (2001).
40. Olive KA, Skillman ED, *Ap. J.* 617:29 (2004), arXiv:astro-ph/0405588.
41. Peimbert A, Peimbert M, Luridiana V, *Ap. J.* 565:668 (2002), arXiv:astro-ph/0107189.
42. Izotov YI, Thuan TX, *Ap. J.* 500:188 (1998).
43. Izotov YI, Thuan TX, *Ap. J.* 602:200 (2004), arXiv:astro-ph/0310421.
44. Bania TM, Rood RT, Balser DS, *Space Sci. Rev.* 130:53 (2007).
45. Vangioni-Flam E, Olive KA, Fields BD, Cassé M, *Ap. J.* 585:611 (2003), arXiv:astro-ph/0207583.
46. Asplund M, Lambert DL, Nissen PE, Primas F, Smith VV, *Ap. J.* 644:229 (2006), arXiv:astro-ph/0510636.
47. Spite F, Spite M, *Astron. Astrophys.* 115:357 (1982).
48. Ryan SG, Norris JE, Beers TC, *Ap. J.* 523:654 (1999), arXiv:astro-ph/9903059.
49. Bonifacio P, Molaro P, Sivarani T, Cayrel R, Spite M, et al., *Astron. Astrophys.* 462:851 (2007), arXiv:astro-ph/0610245.
50. Korn AJ, Grundahl F, Richard O, Barklem PS, Mashonkina L, et al., *Nature* 442:657 (2006), arXiv:astro-ph/0608201.
51. Sbordone L, Bonifacio P, Caffau E, Ludwig H, Behara NT, et al., *Astron. Astrophys.* 522:A26+ (2010), 1003.4510.
52. Aoki W, Barklem PS, Beers TC, Christlieb N, Inoue S, et al., *Ap. J.* 698:1803 (2009), 0904.1448.
53. Hosford A, Ryan SG, García Pérez AE, Norris JE, Olive KA, *Astron. As-*

- trophys. 493:601 (2009), 0811.2506.
54. Hosford A, García Pérez AE, Collet R, Ryan SG, Norris JE, Olive KA, *Astron. Astrophys.* 511:A47+ (2010), 1004.0863.
 55. Meléndez J, Casagrande L, Ramírez I, Asplund M, Schuster WJ, *Astron. Astrophys.* 515:L3+ (2010), 1005.2944.
 56. González Hernández JI, Bonifacio P, Caffau E, Steffen M, Ludwig H, et al., *Astron. Astrophys.* 505:L13 (2009), 0909.0983.
 57. Ryan SG, Beers TC, Olive KA, Fields BD, Norris JE, *Ap. J. Lett.* 530:L57 (2000), arXiv:astro-ph/9905211.
 58. Monaco L, Bonifacio P, Sbordone L, Villanova S, Pancino E, *Astron. Astrophys.* 519:L3+ (2010), 1008.1817.
 59. Cayrel R, Steffen M, Chand H, Bonifacio P, Spite M, et al., *Astron. Astrophys.* 473:L37 (2007), 0708.3819.
 60. Hu W, Dodelson S, *Annu. Rev. Astron. Astrophys.* 40:171 (2002), arXiv:astro-ph/0110414.
 61. Yang J, Turner MS, Schramm DN, Steigman G, Olive KA, *Ap. J.* 281:493 (1984).
 62. Walker TP, Steigman G, Kang H, Schramm DM, Olive KA, *Ap. J.* 376:51 (1991).
 63. Komatsu E, Dunkley J, Nolta MR, Bennett CL, Gold B, et al., *Ap. J. Supp.* 180:330 (2009), 0803.0547.
 64. Fields BD, Olive KA, Vangioni-Flam E, *Ap. J.* 623:1083 (2005), arXiv:astro-ph/0411728.
 65. Meléndez J, Ramírez I, *Ap. J. Lett.* 615:L33 (2004), arXiv:astro-ph/0409383.
 66. Casagrande L, Ramírez I, Meléndez J, Bessell M, Asplund M, *Astron. Astrophys.* 512:A54+ (2010), 1001.3142.
 67. Wallerstein G, Conti PS, *Annu. Rev. Astron. Astrophys.* 7:99 (1969).
 68. Spite M, Spite F, *Annu. Rev. Astron. Astrophys.* 23:225 (1985).
 69. Gustafsson B, *Annu. Rev. Astron. Astrophys.* 27:701 (1989).
 70. Pinsonneault M, *Annu. Rev. Astron. Astrophys.* 35:557 (1997).
 71. Bodenheimer P, *Ap. J.* 142:451 (1965).
 72. Iben Jr. I, *Ap. J.* 147:624 (1967).
 73. Pinsonneault MH, Deliyannis CP, Demarque P, *Ap. J. Supp.* 78:179 (1992).
 74. Talon S, Charbonnel C, *Astron. Astrophys.* 418:1051 (2004), arXiv:astro-ph/0401474.
 75. Richard O, Michaud G, Richer J, *Ap. J.* 619:538 (2005), arXiv:astro-ph/0409672.
 76. Greenstein JL, Richardson RS, *Ap. J.* 113:536 (1951).
 77. Brown L, Schramm DN, *Ap. J. Lett.* 329:L103 (1988).
 78. Malaney RA, Fowler WA, *Ap. J. Lett.* 345:L5 (1989).
 79. Thomas D, Schramm DN, Olive KA, Mathews GJ, Meyer BS, Fields BD, *Ap. J.* 430:291 (1994), arXiv:astro-ph/9308026.
 80. Iocco F, Mangano G, Miele G, Pisanti O, Serpico PD, *Phys. Rev. D* 75:087304 (2007), arXiv:astro-ph/0702090.
 81. Vangioni-Flam E, Coc A, Cassé M, *Astron. Astrophys.* 360:15 (2000), arXiv:astro-ph/0002248.
 82. Boyd RN, Brune CR, Fuller GM, Smith CJ, *Phys. Rev. D* 82:105005 (2010), 1008.0848.
 83. Chakraborty N, Fields BD, Olive KA, ArXiv e-prints (2010), 1011.0722.
 84. Cyburt RH, Davids B, *Phys. Rev. C* 78:064614 (2008), 0809.3240.

85. Cyburt RH, Fields BD, Olive KA, Phys. Rev. D 69:123519 (2004), arXiv:astro-ph/0312629.
86. Dicus DA, Kolb EW, Gleeson AM, Sudarshan ECG, Teplitz VL, Turner MS, Phys. Rev. D 26:2694 (1982).
87. Seckel D, ArXiv High Energy Physics - Phenomenology e-prints (1993), arXiv:hep-ph/9305311.
88. Dolgov AD, Fukugita M, Phys. Rev. D 46:5378 (1992).
89. Kernan PJ, Krauss LM, Physical Review Letters 72:3309 (1994), arXiv:astro-ph/9402010.
90. Dodelson S, Turner MS, Phys. Rev. D 46:3372 (1992).
91. Hannestad S, Madsen J, Phys. Rev. D 52:1764 (1995), arXiv:astro-ph/9506015.
92. Lopez RE, Turner MS, Phys. Rev. D 59:103502 (1999).
93. Esposito S, Mangano G, Miele G, Pisanti O, Nuclear Physics B 540:3 (1999), arXiv:astro-ph/9808196.
94. Smith CJ, Fuller GM, Phys. Rev. D 81:065027 (2010), 0905.2781.
95. Voronchev VT, Nakao Y, Nakamura M, Ap. J. 725:242 (2010).
96. Itoh N, Nishikawa A, Nozawa S, Kohyama Y, Ap. J. 488:507 (1997).
97. Angulo C, Casarejos E, Couder M, Demaret P, Leleux P, et al., Ap. J. Lett. 630:L105 (2005), arXiv:astro-ph/0508454.
98. Cyburt RH, Pospelov M, ArXiv e-prints (2009), 0906.4373.
99. Chakraborty N, Fields BD, Olive KA, ArXiv e-prints (2010), 1011.0722.
100. Hoyle F, Ap. J. Supp. 1:121 (1954).
101. Feng JL, Annu. Rev. Astron. Astrophys. 48:495 (2010), 1003.0904.
102. Hooper D, Baltz EA, Annual Review of Nuclear and Particle Science 58:293 (2008), 0802.0702.
103. Gaitskell RJ, Annual Review of Nuclear and Particle Science 54:315 (2004).
104. Ellis J, Kim JE, Nanopoulos DV, Physics Letters B 145:181 (1984).
105. Lindley D, Ap. J. 294:1 (1985).
106. Ellis J, Nanopoulos DV, Sarkar S, Nuclear Physics B 259:175 (1985).
107. Juskiewicz R, Silk J, Stebbins A, Physics Letters B 158:463 (1985).
108. Kawasaki M, Sato K, Physics Letters B 189:23 (1987).
109. Reno MH, Seckel D, Phys. Rev. D 37:3441 (1988).
110. Scherrer RJ, Turner MS, Ap. J. 331:19 (1988).
111. Dimopoulos S, Esmailzadeh R, Hall LJ, Starkman GD, Nuclear Physics B 311:699 (1989).
112. Ellis J, Gelmini GB, Lopez JL, Nanopoulos DV, Sarkar S, Nuclear Physics B 373:399 (1992).
113. Moroi T, Murayama H, Yamaguchi M, Physics Letters B 303:289 (1993).
114. Jedamzik K, Phys. Rev. D 74:103509 (2006), arXiv:hep-ph/0604251.
115. Cyburt RH, Ellis J, Fields BD, Olive KA, Phys. Rev. D 67:103521 (2003), arXiv:astro-ph/0211258.
116. Kawasaki M, Kohri K, Moroi T, Phys. Rev. D 71:083502 (2005), arXiv:astro-ph/0408426.
117. Pospelov M, Physical Review Letters 98:231301 (2007), arXiv:hep-ph/0605215.
118. Jedamzik K, Phys. Rev. D 70:083510 (2004), arXiv:astro-ph/0405583.
119. Jedamzik K, Phys. Rev. D 70:063524 (2004), arXiv:astro-ph/0402344.
120. Jedamzik K, Choi K, Roszkowski L, Ruiz de Austri R, J. Cosmol. Astropart. Phys. 7:7 (2006), arXiv:hep-ph/0512044.

121. Kusakabe M, Kajino T, Boyd RN, Yoshida T, Mathews GJ, Phys. Rev. D 76:121302 (2007), 0711.3854.
122. Pospelov M, Pradler J, Steffen FD, J. Cosmol. Astropart. Phys. 11:20 (2008), 0807.4287.
123. Jedamzik K, Phys. Rev. D 77:063524 (2008), 0707.2070.
124. Bailly S, Jedamzik K, Moultaqa G, Phys. Rev. D 80:063509 (2009), 0812.0788.
125. Peskin ME, *Supersymmetry in Elementary Particle Physics* (World Scientific, 2008), pp. 609–+.
126. Olive KA, Course 5: Introduction to Supersymmetry: Astrophysical and Phenomenological Constraints, in *The Primordial Universe*, pp. 221–+, 2000, arXiv:hep-ph/9911307.
127. Martin SP, A Supersymmetry Primer, in *Perspectives on Supersymmetry*, pp. 1–+, 1998, arXiv:hep-ph/9709356.
128. Ellis J, Hagelin JS, Nanopoulos DV, Olive K, Srednicki M, Nuclear Physics B 238:453 (1984).
129. Ellis J, Olive KA, Santoso Y, Spanos VC, Physics Letters B 565:176 (2003), arXiv:hep-ph/0303043.
130. Kamimura M, Kino Y, Hiyama E, Progress of Theoretical Physics 121:1059 (2009), 0809.4772.
131. Kusakabe M, Kajino T, Yoshida T, Mathews GJ, Phys. Rev. D 81:083521 (2010), 1001.1410.
132. Bird C, Koopmans K, Pospelov M, Phys. Rev. D 78:083010 (2008), arXiv:hep-ph/0703096.
133. Kusakabe M, Kajino T, Boyd RN, Yoshida T, Mathews GJ, Ap. J. 680:846 (2008), 0711.3858.
134. Cyburt RH, Ellis J, Fields BD, Olive KA, Spanos VC, J. Cosmol. Astropart. Phys. 11:14 (2006), arXiv:astro-ph/0608562.
135. Kawasaki M, Kohri K, Moroi T, Yotsuyanagi A, Phys. Rev. D 78:065011 (2008), 0804.3745.
136. Kohri K, Takahashi T, Physics Letters B 682:337 (2010), 0909.4610.
137. Uzan J, Reviews of Modern Physics 75:403 (2003), arXiv:hep-ph/0205340.
138. Flambaum VV, Shuryak EV, Phys. Rev. D 67:083507 (2003), arXiv:hep-ph/0212403.
139. Flambaum VV, Wirlinga RB, Phys. Rev. C 76:054002 (2007), 0709.0077.
140. Coc A, Nunes NJ, Olive KA, Uzan J, Vangioni E, Phys. Rev. D 76:023511 (2007), arXiv:astro-ph/0610733.
141. Berengut JC, Flambaum VV, Dmitriev VF, Physics Letters B 683:114 (2010), 0907.2288.
142. Coc A, Olive KA, Uzan J, Vangioni E, Phys. Rev. D 79:103512 (2009), 0811.1845.
143. Flambaum VV, Shuryak EV, Phys. Rev. D 65:103503 (2002), arXiv:hep-ph/0201303.
144. Dmitriev VF, Flambaum VV, Webb JK, Phys. Rev. D 69:063506 (2004), arXiv:astro-ph/0310892.
145. Moffat JW, J. Cosmol. Astropart. Phys. 5:1 (2006), arXiv:astro-ph/0505326.
146. Regis M, Clarkson C, ArXiv e-prints (2010), 1003.1043.
147. Holder GP, Nollett KM, van Engelen A, Ap. J. 716:907 (2010), 0907.3919.
148. Piau L, Beers TC, Balsara DS, Sivarani T, Truran JW, Ferguson JW, Ap. J. 653:300 (2006), arXiv:astro-ph/0603553.

149. Fields BD, Olive KA, Silk J, Cassé M, Vangioni-Flam E, *Ap. J.* 563:653 (2001), arXiv:astro-ph/0107389.
150. Vangioni E, Silk J, Olive KA, Fields BD, *ArXiv e-prints* (2010), 1010.5726.

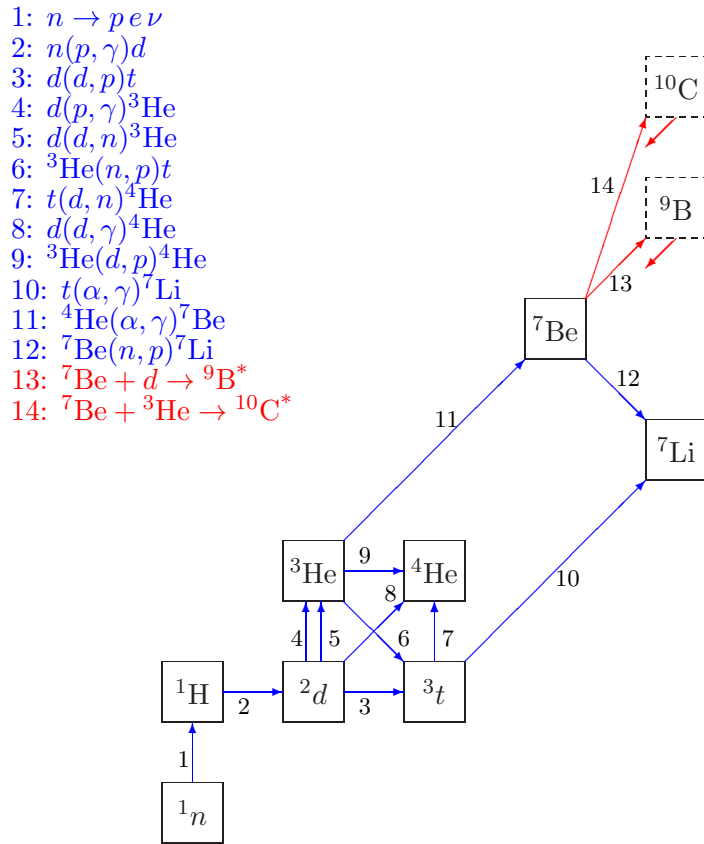


Figure 1: Simplified BBN nuclear network: 12 normally important reactions shown in blue, and proposed/tested new reactions in red.

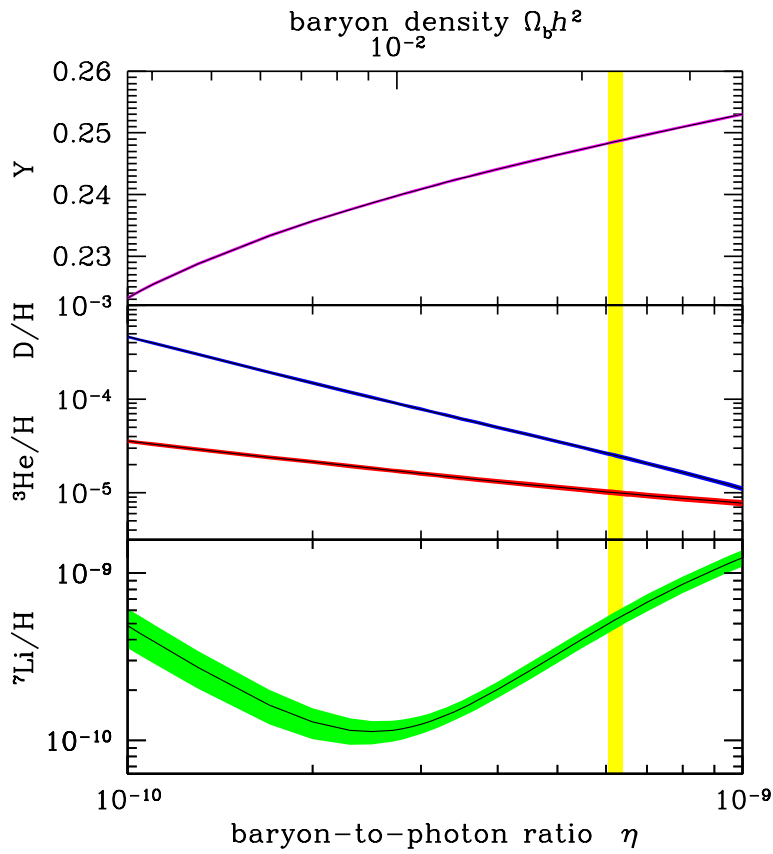


Figure 2: BBN theory predictions for light nuclide abundances vs baryon-to-photon ratio η . Curve widths: 1σ theoretical uncertainties. Vertical band: WMAP determination of η .

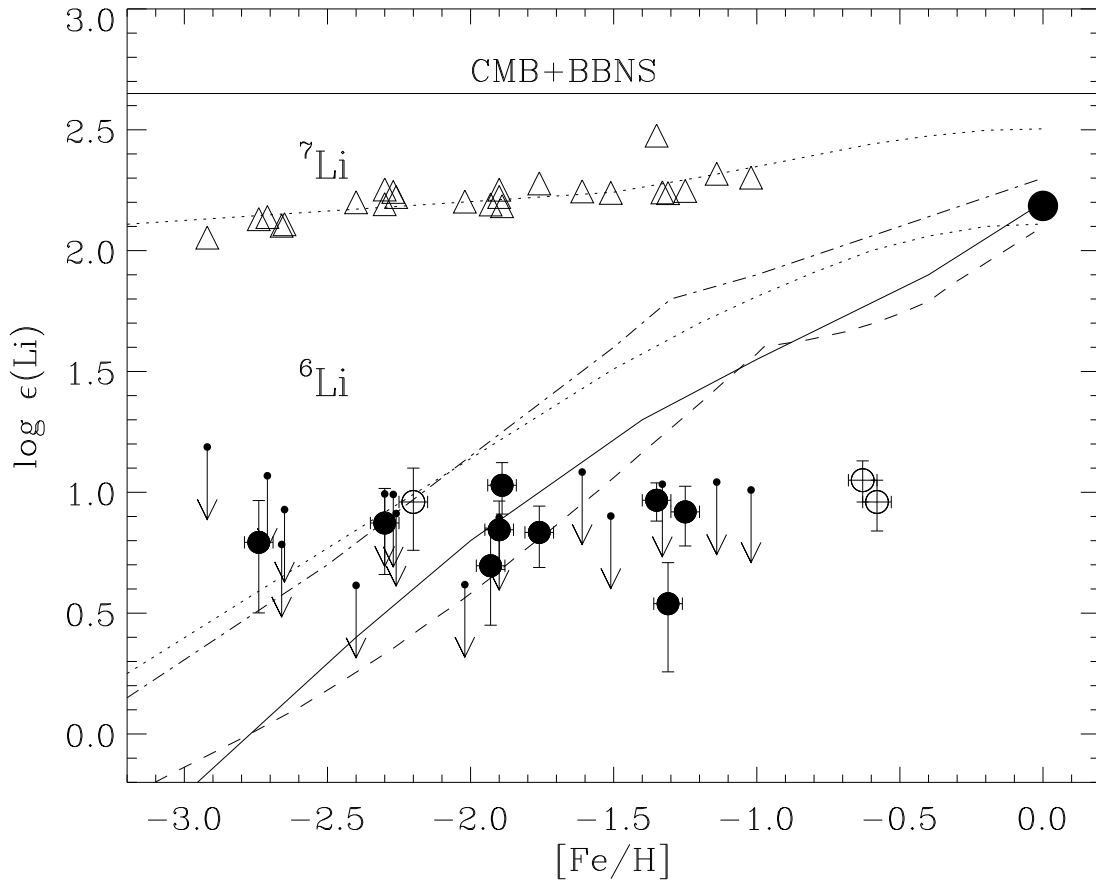


Figure 3: Lithium abundances in selected metal-poor Galactic halo stars, from (46) with permission. For each star, elemental $\text{Li} = {}^6\text{Li} + {}^7\text{Li}$ is plotted at the star's metallicity $[\text{Fe}/\text{H}] = \log_{10}[(\text{Fe}/\text{H})_{\text{obs}}/(\text{Fe}/\text{H})_{\odot}]$. The flatness of Li vs Fe is the “Spite plateau” and indicates that the bulk of the lithium is unrelated to Galactic nucleosynthesis processes and thus is primordial. The horizontal band gives the BBN+WMAP prediction; the gap between this and the plateau illustrates the ${}^7\text{Li}$ problem. Points below the plateau show ${}^6\text{Li}$ abundances; the apparent plateau constitutes the ${}^6\text{Li}$ problem.

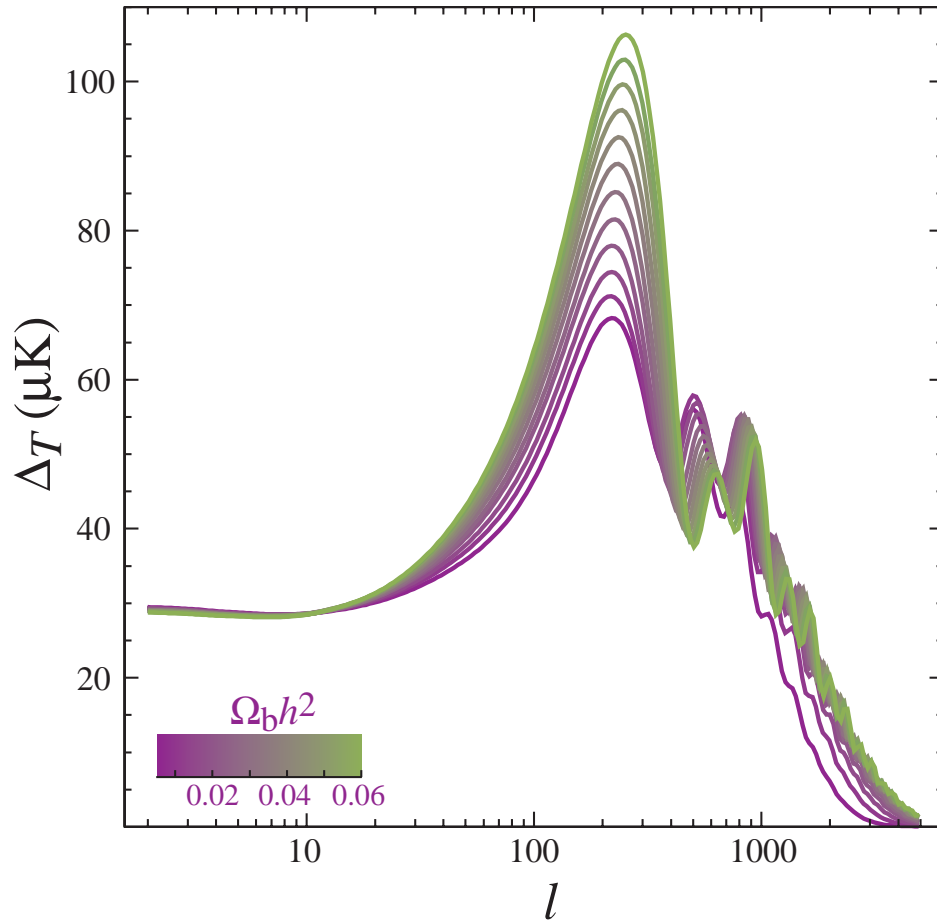


Figure 4: CMB sensitivity to cosmic baryon content. Predictions for temperature anisotropy (rms of temperature fluctuation $\Delta_T^2 = \langle T_\ell^2 \rangle - \langle T \rangle^2$) plotted as a function of angular scale (multipole ℓ , roughly corresponding to angular size $180^\circ/\ell$). Baryon density is seen to be encoded in the values and particularly the ratios of the peak heights. Figure from (60), with permission.

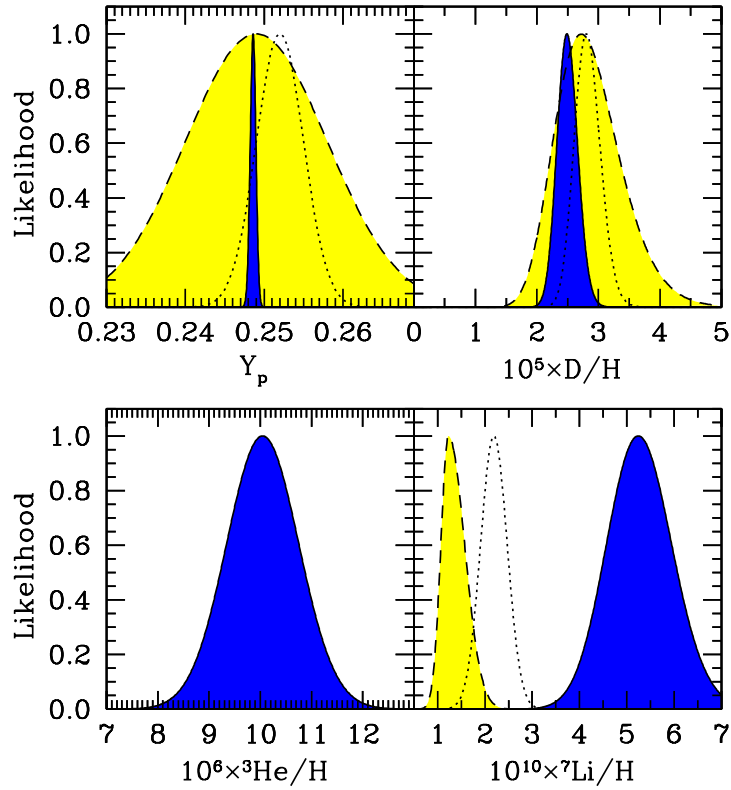


Figure 5: Comparison of BBN+WMAP predictions and observations, from (30). Plotted are likelihood distributions for light nuclide abundances. *Blue curves*: theory likelihoods predicted for standard BBN using the cosmic baryon density determined by WMAP(63). *Yellow curves*: observational likelihoods based on primordial abundances as in §2.2. *Dotted curves*: observational likelihoods for different analyses of abundance data; the difference between these and the yellow curves gives a sense of the systematic errors. Note the spectacular agreement of D/H , and in contrast the strong mismatch between ${}^7\text{Li}$ theory and data, which constitutes the lithium problem.

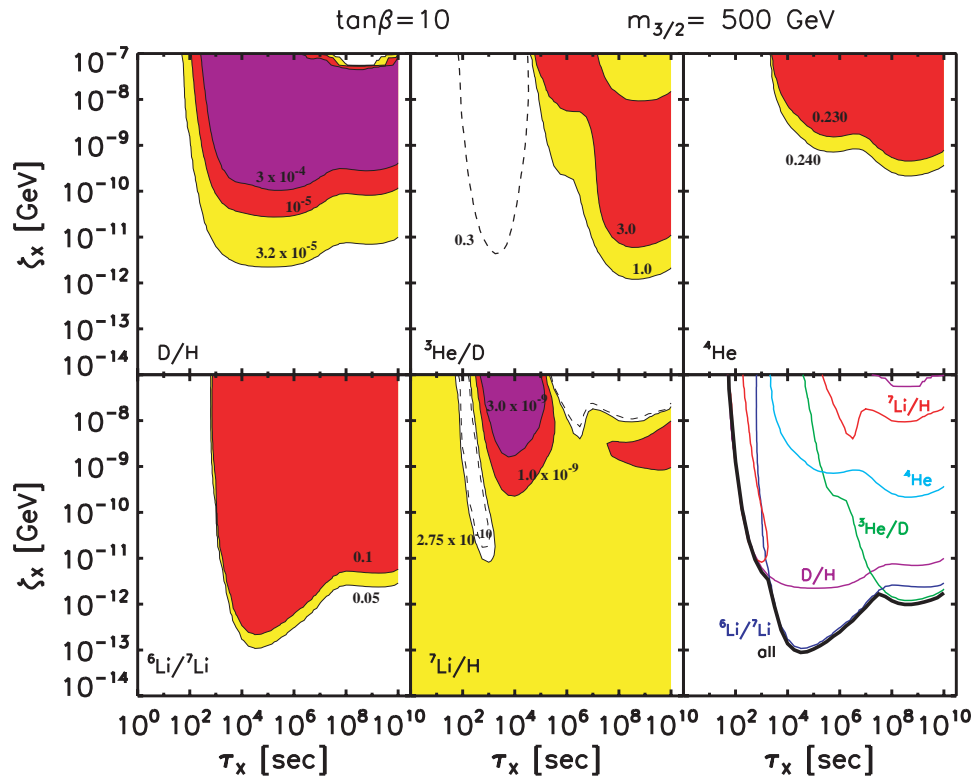


Figure 6: Effect of nonthermal particle injection on light element abundances, from (31). Each panel shows abundance contours in the presence of the hadronic decay of a (neutral) particle X , plotted as a function of X abundance ζ_X (eq. 15) and mean life τ_X . Results are shown for a hadronic branching ratio $B_h = 1$. As summarized in the last panel, the parameter regions where the ${}^7\text{Li}$ problem is solved also lead to deuterium production, placing the two in tension.

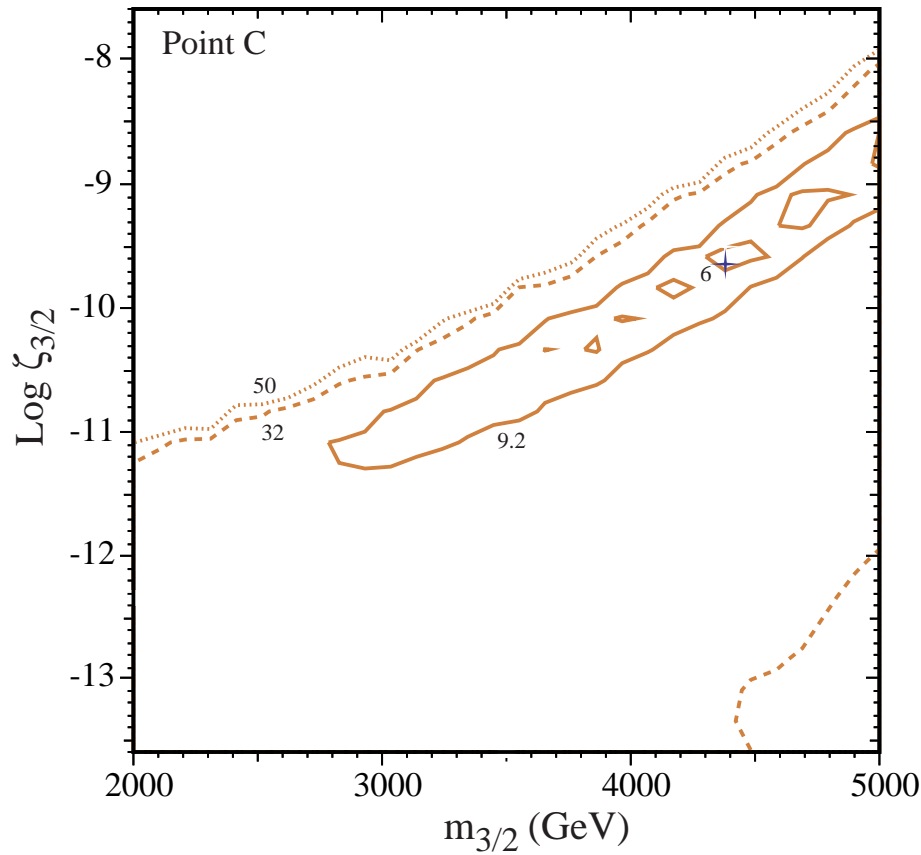


Figure 7: Light element constraints on gravitino decays in the context of the constrained minimal supersymmetric Standard Model, from (32). Shown are χ^2 contours based on light element abundance constraints and 1 effective degrees of freedom, over the space of gravitino mass $m_{3/2}$ and abundance $\zeta_{3/2}$ (eq. 15). The cross indicates the maximum χ^2 . diagonal “archipelago” shows the region where the lithium problem is greatly reduced by trading off ${}^7\text{Li}$ destruction for some degree of deuterium production.